

Revealing missing parts of the interactome

Ryan W. Solava and Tijana Milenković*

Department of Computer Science and Engineering, ECK Institute for Global Health, and
Interdisciplinary Center for Network Science and Applications

University of Notre Dame, Notre Dame, IN 46556, USA

*E-mail: tmilenko@nd.edu

Abstract

Protein interaction networks (PINs) are often used to “learn” new biological function from their topology. Since current PINs are noisy, their computational de-noising via link prediction (LP) could improve the learning accuracy. LP uses the existing PIN topology to predict missing and spurious links. Many of existing LP methods rely on shared *immediate* neighborhoods of the nodes to be linked. As such, they have limitations. Thus, in order to *comprehensively* study what are the topological properties of nodes in PINs that dictate whether the nodes should be linked, we had to introduce novel *sensitive* LP measures that overcome the limitations of the existing methods.

We systematically evaluate the new and existing LP measures by introducing “synthetic” noise to PINs and measuring how well the different measures reconstruct the original PINs. Our main findings are: 1) LP measures that favor nodes which are *both* “topologically similar” *and* have large shared *extended* neighborhoods are superior; 2) using more network topology often though not always improves LP accuracy; and 3) our new LP measures are superior to the existing measures. After evaluating the different methods, we use them to de-noise PINs. Importantly, we manage to improve biological correctness of the PINs by de-noising them, with respect to “enrichment” of the predicted interactions in Gene Ontology terms. Furthermore, we validate a statistically significant portion of the predicted interactions in independent, external PIN data sources.

Software executables are freely available upon request.

Introduction

Motivation and background

Networks (or graphs) model real-world phenomena in many domains. We focus on biological networks, protein-protein interaction (PPI) networks in particular, with the goal of identifying missing and spurious links in current noisy PPI networks. Nonetheless, our study is applicable to other network types as well. In PPI networks, nodes are proteins and two nodes are connected by an edge if the corresponding proteins interact in the cell. We focus on these networks, since it is the proteins (gene products) that carry out the majority of cellular processes and they do so by interacting with other proteins. And this is exactly what PPI networks model.

High-throughput methods for PPI detection, e.g., yeast two-hybrid (Y2H) assays or affinity purification followed by mass spectrometry (AP/MS), have produced PPI data for many species [10, 40, 47, 38, 4]. However, current networks are *noisy*, with many missing and spurious PPIs, due to limitations of biotechnologies as well as human biases [44, 41, 11, 6, 46]. AP/MS is estimated to have a 15-50% false positive rate and a 63-77% false negative rate [8]. Similar holds for Y2H, though PPIs obtained by Y2H are still more precise than literature-curated PPIs supported by a single publication [43].

Analogous to genomic sequence research, biological network research is promising to revolutionize our biological understanding: prediction of protein function and the role of proteins in disease from PPI network topology has already received much attention [35, 37, 36, 3, 42]. However, the noisiness of the network data is an obstacle on this promising avenue, as it could lead to incorrect predictions. Computational de-noising of current PPI network data by identifying missing and spurious links could

improve the quality of topology-based predictions and consequently save resources needed for experimental validation of the predictions. Hence, we aim to test how well we can decrease the noise in PPI data via link prediction (LP).

LP typically uses the existing topology of the network to predict missing and spurious links [16, 9, 17, 18, 20, 32, 34]. Alternatively, one network type, e.g., functional interactions, can be used to predict another network type, e.g., physical PPIs [34]. LP consists of unsupervised or supervised approaches that use some measure of the topology of the nodes to be linked [18]. For example, it may be desirable to link nodes with high degrees as measured by preferential attachment [29], nodes that share many neighbors as measured by Jaccard [33] or Adamic/Adar coefficients [1], or “important” nodes that interact with many other “important” nodes as measured by PageRank [5]. Both supervised and unsupervised LP methods have their (dis)advantages. Though supervised methods can outperform unsupervised ones, much of previous research has focused on unsupervised LP, since many factors that might influence supervised LP have not been well understood [18, 16, 20].

There are some limitations to the existing LP measures. While many capture only the topological information contained in the *immediate* network neighborhood of nodes to be linked, significant amount of the information is available in the rest of the network that could improve LP accuracy. Hence, more sensitive measures that capture deeper network topology are needed. We recently generalized the idea of shared immediate neighborhoods to shared *extended* neighborhoods in the context of network clustering and showed that including more network topology resulted in biologically superior clusters [39]. So, it is reasonable to test whether including more topology will be effective for LP as well.

Also, existing shared neighborhood-based measures can predict a link only between nodes that are within the shortest path *distance of two* from each other, whereas it might be beneficial to link nodes which are *more distant*. Preferential attachment-based measures can achieve this, but they again capture only the immediate neighborhoods of the nodes to be linked. A shortest path-based LP method exists which can also connect distant nodes in the network but which can at the same time capture deeper network topology. However, this method is computationally expensive [15]. Hence, we introduce a sensitive measure of the topological similarity of *extended* neighborhoods of two nodes that addresses all of the above issues, and we use it with the hypothesis that nodes that are topologically similar should be linked together.

Another drawback of the existing methods is as follows. It might be more efficient to predict the existence of a link between two nodes by explicitly measuring the topological position of an *edge* (or equivalently a non-edge) rather than by measuring the position of each of the two *nodes* individually, as the current methods do [19]. Thus, we propose a new, sensitive measure of the network position of an *edge* and a *non-edge*, which counts the number of subgraphs that the two nodes in question participate in *simultaneously*, and we use it with the hypothesis that nodes that participate in many subgraphs and thus have large and dense *extended* shared neighborhoods should be linked together.

Our approach

We study several PPI networks of yeast, the best studied species to date, obtained by different experimental methods for PPI detection, and we apply our new as well as commonly used existing LP measures to the networks to de-noise them. Given a network, we aim to study the topologies of each node pair in the network with respect to the given LP measure, in order to determine which of the node pairs should be connected. We compare the different LP methods in systematic receiver-operator curve and precision-recall settings. For each of the two method comparison settings, we perform two types of evaluation tests. First, we introduce synthetic noise in the given PPI network by randomly removing a percentage of edges from the network, with the goal of measuring how well the given method can reconstruct the original network, using the original PPIs as the ground truth data. Second, given the availability of low-confidence PPI data for one of the studied networks, we apply the given method to this network and use the corresponding low-confidence PPI data as the ground truth data when evaluating the method.

We study the effects on LP accuracy of the “topological similarity” as well as size of the shared *extended* neighborhoods of nodes, where the nodes *can* be distant in the network. Also, we study what amount of network topology should be used for LP. We find that LP measures which favor nodes which are *both* topologically similar and which have large shared extended neighborhoods are superior. We show that using more network topology often though not always increases LP accuracy. Importantly, we show that our new LP measures are statistically significantly superior to the existing ones. Alarming, we find that receiver-operator curve and precision-recall method comparison frameworks do not necessarily agree, which has important implications for the LP community.

After we evaluate the different methods, we apply the methods to the PPI networks to de-noise them, and we evaluate the quality of the de-noised networks in two ways. First, we compute their biological correctness by measuring the “enrichment” of predicted edges in Gene Ontology (GO) terms [2]. Importantly, we show that our new LP measures as well as some of the existing measures improve the biological correctness of the PPI networks by de-noising them. Second, we search for the predicted interactions in an external, independent PPI data source, and in this way, we validate a significantly large portion of the predictions, further confirming the biological correctness of the de-noised networks.

Methods

We study multiple *S. cerevisiae* PPI networks obtained by different experimental methods for PPI detection. Given a network, we aim to de-noise the network, with the goal of determining which of all pairs of nodes in the network should be connected by edges, with respect to a variety of existing as well as new LP measures. We evaluate the different measures in systematic precision-recall and receiver-operator curve frameworks. The details are as follows.

Network data

We evaluate all LP methods on three *S. cerevisiae* yeast PPI networks obtained with different experimental methods. We study PPI networks of *yeast* because yeast has been the most studied species to date. As such, it has the most complete interactome and thus represents the best species to evaluate the methods on. We study *multiple* yeast PPI networks obtained with *different* experimental methods for PPI detection to test whether LP results are dependent on the experimental method. The three networks are: 1) *Y2H* network, obtained by Y2H, which consists of 1,647 nodes and 2,518 edges [47, 39]; 2) *AP/MS* network, obtained by AP/MS, which consists of 1,004 nodes and 8,319 edges [47, 39]; and 3) *high-confidence (HC)* network, obtained from multiple data sources, which consists of 1,004 nodes and 8,323 edges [6]. The quality of PPIs in the HC network is comparable to the quality of interactions produced by precise small-scale biological experiments [6]. Importantly, in addition to the high-confidence PPIs, the data by [6] also contains the corresponding lower-confidence PPI data, which is useful for evaluation of the LP methods (as explained below).

Existing commonly used LP measures

Degree-based measure

According to preferential attachment [29], the higher the degrees of two nodes, the more likely the nodes are to interact. The *degree product (DP)* measure scores the potential edge between two nodes v and w as: $DP(v, w) = d(v) \times d(w)$, where $d(v)$ is the degree of node v [18].

Common neighbors-based measures

A popular idea is that the more neighbors two nodes share, the more likely the nodes are to interact.

The *shared neighbors (SN)* measure scores the potential edge between nodes v and w as: $SN(v, w) = |N(v) \cap N(w)|$, where $N(v)$ is the set of neighbors of v [29]. SN simply counts the shared neighbors.

Jaccard coefficient (JC) scores the potential edge between two nodes v and w as: $JC(v, w) = \frac{|N(v) \cap N(w)|}{|N(v) \cup N(w)|}$ [33]. That is, it scores two nodes with respect to the size of their shared neighborhood relative to the size of their entire neighborhoods combined. As such, it favors node pairs for which a high percentage of all neighbors are shared.

The *Adamic-Adar (AA)* measure scores the potential edge between two nodes v and w as: $AA(v, w) = \sum_{z \in N(v) \cap N(w)} \frac{1}{d(z)}$ [1]. Thus, of all common neighbors of two nodes, it favors low-degree shared neighbors over high-degree shared neighbors.

New LP measures

We already designed sensitive measures of topology that unlike the existing measures go beyond capturing only the direct neighborhoods of nodes to be linked. We used them for network alignment [13, 27, 14], clustering [28, 25, 12, 39], and modeling [22, 23], but they have not been used for LP thus far. Thus, we introduce them as new LP measures. Also, we design conceptually new measures. The details are as follows.

Existing sensitive measures of topology as new LP measures

To go beyond capturing only the direct network neighborhood of a node, we previously designed a constraining graphlet-based measure of topology, called *node graphlet degree vector (node-GDV)*, that captures up to 4-deep neighborhood of a node; a graphlet is a small induced subgraph of the network [31]. We designed a measure of topological similarity of such extended neighborhoods of two nodes, called *node-GDV-similarity*. In this study, we use node-GDV-similarity for LP, with the hypothesis that the more topologically similar two nodes are, the more likely the nodes are to interact. Also, since shared neighbors-based approaches, which are among the best LP measures over the widest range of real-world networks [18], are based on the number of 3-node paths that two nodes in question share, where a 3-node path is just a 3-node graphlet, we generalize these measures by counting the number of all 3-5-node graphlets that the two nodes share. We do this by using a sensitive measure called *edge-GDV*. The formal description of all of the measures is as follows.

Node graphlet degree vector (node-GDV). We generalized the degree of node v that counts the number of edges that v touches (where an edge is the only 2-node graphlet, denoted by G_0 in Fig. 1), into *node-GDV* of v that counts the number of 2-5-node graphlets that v touches [28]. We need to distinguish between v touching, for example, a three-node path (G_1 in Fig. 1) at an end node or at the middle node, because the end nodes are topologically identical to each other, while the middle node is not. This is because an automorphism (defined below) of G_1 maps the end nodes to one another and the middle node to itself. Formally, an isomorphism f from graph X to graph Y is a bijection of nodes of X to nodes of Y such that xy is an edge of X if and only if $f(x)f(y)$ is an edge of Y . An automorphism is an isomorphism from X to itself. The automorphisms of X form the automorphism group, $\text{Aut}(X)$. If x is a node of X , then the automorphism node orbit of x is $\text{Orb}_n(x) = \{y \in V(X) | y = f(x) \text{ for some } f \in \text{Aut}(X)\}$, where $V(X)$ is the set of nodes of X . There are 73 node orbits for 2-5-node graphlets. Hence, node-GDV of v has 73 elements counting how many node orbits of each type touch v (v 's degree is the first element). It captures v 's up to 4-deep neighborhood and thus a large portion of real networks, as they are small-world [45].

Node-GDV-similarity. To compare node-GDVs of two nodes, one could use some existing measure, e.g., Euclidean distance. However, this might be inappropriate, as some orbit counts are not independent. Hence, we designed a new measure, called node-GDV-similarity, as follows [28]. For a node $u \in G$, u_i is the i^{th} element of its node-GDV. The distance between the i^{th} orbits of nodes u and v is $D_i(u, v) =$

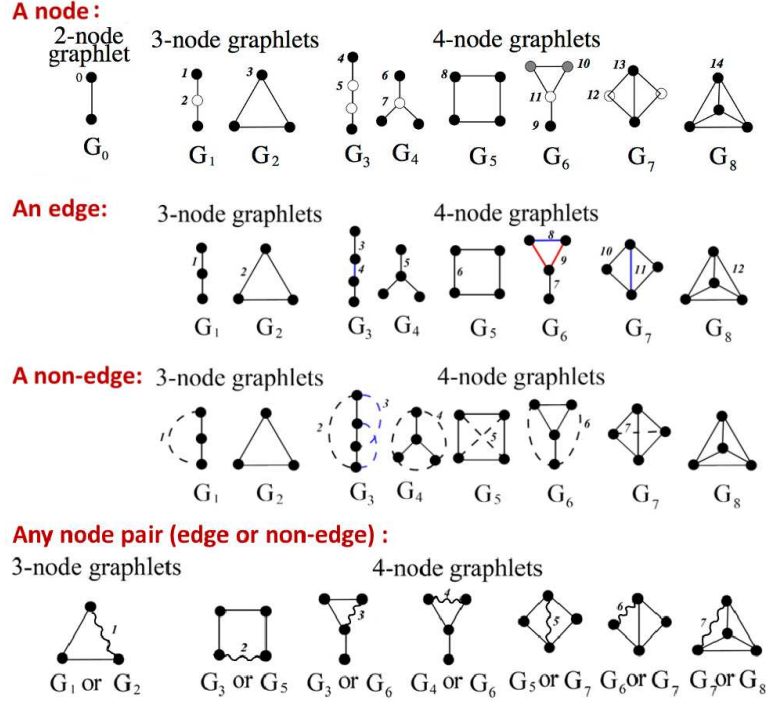


Figure 1. Graphlet positions of a node, an edge, a non-edge, and a node pair. All topological positions (“orbits”) in up to 4-node graphlets of a node (top; node shade), an edge (upper middle; solid line), a non-edge (lower middle; broken line), and any node pair, an edge or a non-edge (bottom; wavy line) are shown. For example: 1) in graphlet G_3 , the two end nodes are in node orbit 4, while the two middle nodes are in node orbit 5; 2) in G_3 , the two “outer” edges are in edge orbit 3, while the “middle” edge is in edge orbit 4; 3) in G_3 , the non-edge touching the end nodes is in non-edge orbit 2, while the two non-edges that touch the end nodes and the middle nodes are in non-edge orbit 3; 4) a node pair at node pair orbit 1 touches a G_2 at edge orbit 2, if it is an edge, or a G_1 at non-edge orbit 1, if it is a non-edge (hence, mutually exclusive edge orbit 2 and non-edge orbit 1 are reconciled into a common node pair orbit 1). There are 15 node, 12 edge, 7 non-edge, and 7 node pair orbits for up to 4-node graphlets. In a graphlet, different orbits are colored differently. All up to 5-node graphlets are used, but only up to 4-node graphlets are illustrated. There are 73 node, 68 edge, 49 non-edge, and 49 node pair orbits for up to 5-node graphlets.

$w_i \times \frac{|\log(u_i+1)-\log(v_i+1)|}{\log(\max\{u_i, v_i\}+2)}$, where w_i is the weight of orbit i that accounts for orbit dependencies [28]. The \log is used because the i^{th} elements of two node-GDVs can differ by several orders of magnitude and we did not want the distance between node-GDVs to be dominated by large values. The total distance is $D(u, v) = \frac{\sum_{i=0}^{72} D_i}{\sum_{i=0}^{72} w_i}$. Finally, node-GDV-similarity is $S(u, v) = 1 - D(u, v)$. The higher the node-GDV-similarity between nodes, the higher their topological similarity.

Edge-GDV. Since a graphlet contains both nodes *and* edges, we defined *edge-GDV* to count the number of graphlets that an *edge* touches at a given “edge orbit” (Fig. 1) [39]. Given the automorphism group of graph X , $\text{Aut}(X)$, if xy is an edge of X , the edge orbit of xy is $\text{Orb}_e(xy) = \{zw \in E(X) | z = f(x) \text{ and } w = f(y) \text{ for some } f \in \text{Aut}(X)\}$, where $E(X)$ is the set of edges of X . There are 68 edge orbits for 3-5-node graphlets [39]. (We designed *edge-GDV-similarity* to measure topological similarity of *edges*,

which we used for network clustering [39]. However, we do not use this measure for LP.)

Conceptually novel measures of topology

We need to predict the existence of a link between nodes independent on whether there is an edge between them in the original network or not. Thus, in addition to describing the network position of an edge, we need to be able to describe the position of a non-edge as well. Hence, we generalize edge-GDV into *non-edge-GDV* to measure the topological position of a non-edge. Then, we reconcile mutually exclusive edge-GDVs and non-edge-GDVs into a new *node-pair-GDV* measure, which counts the number of graphlets that a node pair (an edge or a non-edge) touches at a given “node pair orbit” (defined below). Finally, based on node-pair-edge-GDV of a node pair, we create a new measure of the topological centrality of the node pair, called *node-pair-GDV-centrality*. According to this measure, the more graphlets the two nodes participate in (or share), the higher their centrality. Then, node-pair-GDV-centrality is used as a LP measure to score potential edges between node pairs in the network. The measures are defined as follows.

Non-edge-GDV. Analogous to edge-GDV, in this study, we define *non-edge-GDV* to count the number of graphlets that a *non-edge* touches at a given “non-edge orbit” (Fig. 1). We define non-edge orbits as follows. If xy is a non-edge of graph X , then the non-edge orbit of xy is $\text{Orb}_{ne}(xy) = \{zw \in C(X) | z = f(x) \text{ and } w = f(y) \text{ for some } f \in \text{Aut}(X)\}$, where $C(X)$ is the set of all non-edges of X . For example, in Fig. 1, in graphlet G_1 , the only non-edge is in non-edge orbit 1. Graphlet G_2 has no non-edges. In graphlet G_3 , the non-edge that touches the two end nodes is in one non-edge orbit (non-edge orbit 2), while the remaining two non-edges that touch the end nodes and the middle nodes are in a different non-edge orbit (non-edge orbit 3). And so on. There are 49 non-edge orbits for 3-5-node graphlets.

Node-pair-edge-GDV. Edge and non-edge orbits are mutually exclusive (Fig. 1). However, to perform LP, we need to contrast the topological neighborhood of nodes v and u against the neighborhood of nodes s and t , while hiding the information about whether v and u or s and t are actually linked. Hence, we need to reconcile edge orbits and non-edge orbits by defining *node-pair-GDV* to count the number of graphlets that a general *node pair*, which can be either an edge or a non-edge, touches at a given “node pair orbit”. For example, in Fig. 1, a node pair at node pair orbit 1 touches a triangle (graphlet G_2) at edge orbit 2, if the node pair is an edge, or it touches a three-node path (graphlet G_1) at non-edge orbit 1, if the node pair is a non-edge. Hence, we reconcile mutually exclusive edge orbit 2 and non-edge orbit 1 into a common node pair orbit 1. We do this for all edge- and non-edge orbits, resulting in 49 node pair orbits for 3-5-node graphlets.

Node-pair-GDV-centrality. We design *node-pair-GDV-centrality* to assign high centrality values to node pairs that participate in many graphlets. For nodes v and u , if c_i is the i^{th} element of node-pair-GDV of the two nodes, then $\text{node-pair-GDV-centrality}(vu) = \sum_{i=0}^{49} w_i \times \log(c_i + 1)$. Thus, the more graphlets a node pair participates in, the higher its centrality. Note that we previously designed an analogous measure of the network centrality of a node, called node-GDV-centrality [26].

Using the new measures for LP

Node-GDV-similarity and node-pair-GDV-centrality measures allow for several simple modifications which could perhaps improve LP accuracy, as follows.

Combining node-GDV-similarity and node-pair-GDV-centrality. Node-GDV-similarity favors linking topologically similar nodes. Node-pair-GDV-centrality favors linking nodes that share many graphlets. Combining the two would favor linking nodes that are *both* topologically similar and share many graphlets. We combine them as: $(1 - \alpha) \times \text{node-GDV-similarity} + \alpha \times \text{node-pair-GDV-centrality}$. We vary α from 0 to 1 in increments of 0.2.

Prioritizing dense graphlets. Node-pair-GDV-centrality, as defined above, counts the number of graphlets that two nodes share, while assigning weights to different graphlets only with respect to “orbit dependencies” (see [28] for details). However, it ignores any information about the *denseness* of the graphlets that the two nodes share. Analogous to Adamic-Adar which favors some shared neighbors over others based on their degrees (see above), we might want to favor some shared graphlets over others based on their denseness. For example, it might be more reasonable to link two nodes that share many 4-node cliques than two nodes that share many 4-node paths. So, we favor denser shared graphlets over sparser shared graphlets by defining *density-weighted* (or simply *weighted*) *node-pair-GDV-centrality* (Supplementary Section S1). We evaluate both unweighted and weighted node-pair-GDV-centrality measures.

Graphlet size. To test how much of network topology is beneficial for LP, when using the graphlet-based measures, we use: 1) all 3-5-node graphlets, 2) 3-4-node graphlets, but not 5-node graphlets, and 3) only 3-node graphlets. Note that using the only 3-node graphlet within the node-pair-GDV-centrality at α of 1 (see above) is equivalent to the SN measure (see above). Hence, SN is a variation of node-pair-GDV-centrality. Also, note that when using 3-node graphlets, unweighted and weighted node-pair-GDV-centralities are equivalent. This is because there is only one 3-node graphlet when dealing with node-pair-GDVs, and its density is one. Determining which amount of topology to use is important: the more topology (the larger the graphlets), the higher the computational complexity. Exhaustive counting of all graphlets on up to n nodes in graph $G(V, E)$ takes $O(|V|^n)$; but, the practical running time is much smaller due to the sparseness of real networks [24, 30, 21]. Also, counting is embarrassingly parallel. Finally, fast non-exhaustive approaches exist for counting graphlets [21].

Evaluation framework

We evaluate each of the existing and new LP methods on each of the PPI networks as follows.

First, we introduce synthetic noise in the given PPI network by randomly removing 5%-50% of its edges, with the goal of measuring how well the different methods can reconstruct the original network, using the original PPIs as the ground truth data. We apply the given LP measure to a “noisy” network created in this way and score each node pair in the network, so that the higher the score, the more likely the nodes are to be linked. We predict $k\%$ of the highest-scoring node pairs as edges. We vary k from 0% to 100% in increments of 1%. At each k , we count the number of true positives, true negatives, false positives, and false negatives, and we compute: 1) precision, recall, and F-score; and 2) sensitivity and specificity (Supplementary Section S2) [7]. For simplicity of comparing results across different methods, we summarize the performance of the methods over the entire range of k with respect to sensitivity and specificity by calculating the areas under receiver-operator curves (AUROCs).

To account for randomness in the above procedure, for each level of noise, we randomly remove the given percentage of edges from the original network five times and average the above statistics over the five runs. Ideally, we would perform more random runs, but this is impractical due to the required computational time. Plus, this might be unnecessary, since the standard deviations resulting from the five runs are typically very small (Section “Results and Discussion”), and since even with five random runs of each method, we can compute the statistical significance of the difference in LP accuracy between a pair of methods by using the *paired t*-test. With this test, we compare five pairs of AUROCs corresponding to five random runs of two methods, and a low p -value would indicate that the null hypothesis (the difference between the accuracy of the two methods having a mean of 0) can be rejected.

Second, due to the availability of low-confidence PPI data for the HC network (see above), we perform an additional evaluation test: we apply the given LP method to the HC network and use the low-confidence PPIs as the ground truth data. We evaluate the method in the same way as above.

Third, we apply the given LP method to a network to de-noise it, and we evaluate the biological quality of the de-noised network with respect to the “enrichment” of predicted edges in Gene Ontology

(GO) terms [2]. We compute the enrichment as the percentage of predicted edges, out of all edges in which both proteins have at least one GO term, in which the two end nodes share a GO term. As [15], we do this for biological process GO terms. To avoid potential biases, we consider only gene-GO term associations with experimental evidence codes. Since we de-noise networks by relying on their topology (i.e., on the PPIs), to avoid “circular arguments”, of these associations, we exclude associations inferred from PPIs. We compute the statistical significance of the enrichment by using the hypergeometric model (Supplementary Section S2).

Finally, we validate predicted edges absent from the original network by searching for them in an independent PPI data source. Here, we use BioGRID [4], because it is a trusted PPI data source. Again, we measure the statistical significance of validating the given number of predictions by using the hypergeometric model (Supplementary Section S2). We perform the external data source validation on AP/MS predictions as this network uses the same naming scheme as BioGRID.

Results and Discussion

We study three yeast PPI networks: AP/MS, Y2H, and HC. We use a number of existing and new LP measures. The existing measures are degree product (DP), shared neighbors (SN), Jaccard coefficient (JC), and Adamic-Adar (AA). The new measures are node-GDV-similarity and node-pair-GDV-centrality. See Methods for details.

The two graphlet-based measures allow us to address several important LP questions. First, we can combine node-GDV-similarity, which favors linking nodes with topologically similar neighborhoods, with node-pair-GDV-centrality, which favors linking nodes that share many graphlets and thus have large *extended* shared neighborhoods, to favor linking nodes that are *both* topologically similar and share many graphlets, which might be preferred. To test whether this is the case, we combine the two measures by varying the value of parameter α from 0 to 1, where α of 0 means that only node-GDV-similarity is used, and α of 1 means that only node-pair-GDV-centrality is used (see Methods). Second, we test whether favoring denser graphlets that are shared between the nodes in question within the node-pair-GDV-centrality measure is preferred over equally favoring all graphlets, independent on their density. We do this by evaluating both unweighted and weighted node-pair-GDV-centrality measures (see Methods). Third, to test how much of network topology is beneficial for LP, when using the graphlet-based measures, we use: 1) all 3-5 node graphlets, 2) only 3-4-node graphlets, and 3) only 3-node graphlets.

After we compare the different variations of graphlet-based measures, we evaluate the best of them against the existing measures. All methods are evaluated fairly and systematically in AUROC and precision-recall settings (see Methods). We perform two evaluation tests: 1) we introduce synthetic noise in the given PPI network by randomly removing a percentage of its edges, with the goal of measuring how well the given method can reconstruct the original network, using the original PPIs as the ground truth data; and 2) given the availability of low-confidence PPI data corresponding to the HC network, we apply the given LP method to the original HC PPI network and use the corresponding low-confidence PPI data as the ground truth data when evaluating the method (see Methods and below for details).

After we *evaluate* the methods, we *apply* them to the PPI networks to de-noise them, and we evaluate biological quality of the de-noised networks: 1) with respect to the “enrichment” of predicted edges in GO terms [2], and 2) by validating predicted edges in an external data source (see Methods and below for details). Ultimately, we are less focused on identifying a superior LP method but more on testing whether we can de-noise a network so that the de-noised network is biologically more meaningful than the original one, as well as on which topological properties affect LP accuracy.

Evaluating LP methods by introducing synthetic noise into PPI networks

Current PPI networks are noisy. The correct and complete ground truth interactomes are unknown. Thus, an alternative ground truth data has to be sought. We create synthetic ground truth data from the real PPI networks. For each PPI network, we add synthetic noise to the network by randomly removing 5%, 10%, 15%, 20%, 25%, and 50% of the original edges. Then, we evaluate the given LP method by applying it to a synthetically noised network and by measuring how well it reconstructs the original network (see Methods).

Combining topological similarity and centrality of nodes to be linked improves LP accuracy

By combining node-GDV-similarity and node-pair-GDV-centrality with parameter α (see Methods), we find that nodes that are simultaneously topologically similar and share many graphlets are preferred for LP. In general, the larger the value of α (the more node-pair-GDV-centrality is used), the better the LP accuracy (Fig. 2 A). This suggests that the topological similarity of two nodes is less relevant for LP than the number of graphlets that the nodes share. However, using a small amount of node-GDV-similarity in the combined LP score ($\alpha = 0.8$) actually improves LP accuracy compared to using node-pair-GDV-centrality alone ($\alpha = 1$), implying that topological similarity *is* relevant. The difference between LP accuracy of the best α of 0.8 and any other α in Fig. 2 A is statistically significant, with p -values below 2.5×10^{-6} for 5% noise and below 2.8×10^{-4} for 50% noise.

While the results in Fig. 2 A are for weighted node-pair-GDV-centrality, 3-5-node graphlets, two noise levels, and the AP/MS network, in general, they also hold for weighted node-pair-GDV-centrality, all graphlet sizes, all noise levels, and HC and Y2H networks (Supplementary Fig. S1 and S2). And since $\alpha = 0.8$ is statistically significantly superior to all other α s, in the rest of the section, we focus only on this value of α .

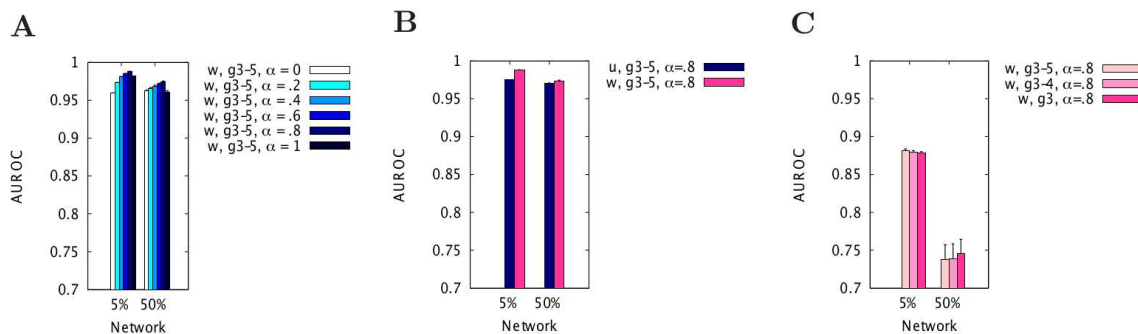


Figure 2. LP accuracy of the graphlet-based methods. The accuracy is shown in terms of AUROCs at the lowest noise level of 5% and the highest noise level of 50% when comparing: **A)** varying α s in the AP/MS network; **B)** unweighted (“u”) vs. weighted (“w”) node-pair-GDV-centrality in the HC network; and **C)** different graphlet sizes (3-5-node (“g3-5”), 3-4-node (“g3-4”), and 3-node (“g3”) graphlets) in the Y2H network. Note that we intentionally vary the networks between panels (AP/MS in panel A, HC in panel B, and Y2H in panel C), but only in order to represent each of the three studied networks equally; we show full results in Supplementary Fig. S1-S4.

Favoring denser shared graphlets improves LP accuracy

We find that preferring denser graphlets (see Methods) improves the LP performance: weighted node-pair-GDV-centrality outperforms the unweighted version (Fig. 2 B), and its superiority is statistically

significant, with p -value of 1.76×10^{-8} for 5% noise and 1.8×10^{-5} for 50% noise.

While the results in the figure are for all 3-5-node graphlets, two noise levels, and the HC network, in general, they also hold for all graphlet sizes, noise levels, and AP/MS and Y2H networks (Supplementary Fig. S3). Thus, henceforth, we focus only on the superior weighted version of node-pair-GDV-centrality.

Using more topology does not always guarantee higher LP accuracy

There is no clear trend on how much topology is best (Fig. 2 C). For example, for the lowest noise level of 5%, using 3-5-node graphlets is statistically significantly superior over using 3-4-node or 3-node graphlets, with p -values of 5.8×10^{-3} and 1.1×10^{-2} , respectively. On the other hand, for the highest noise level of 50%, using 3-5-node graphlets is marginally superior over using 3-4-node graphlets, with p -value of 5.6×10^{-2} , and it is statistically significantly superior over using 3-3-node graphlets, with p -value of 8.6×10^{-3} . Hence, using more network topology can improve LP accuracy, but it is not guaranteed to do so.

Whereas the results in Fig. 2 C are only for two noise levels and the Y2H network, in general, they also hold for other noise levels and for AP/MS and HC networks (Supplementary Fig. S4).

Because in some cases using only 3-node graphlets is superior, and because the existing shared neighbors-based methods and SN in particular also rely on 3-node graphlets (see Methods), one might incorrectly assume that in these cases, our graphlet-based methods do not improve upon the existing methods. However, it is at α of 1 when our node-pair-GDV-centrality and existing SN method are equivalent (see Methods). Since our results at α of 0.8 are superior over results at α of 1 (see above), and since at α of 0.8 SN is actually combined with graphlet information encoded in the node-GDV-similarity measure, node-GDV-similarity actually *improves* the accuracy of SN even when using 3-node graphlets only and especially when using all 3-5-node graphlets is superior to using only 3-node graphlets.

Also, using deeper network topology is superior to using only the direct network neighborhood of nodes to be linked in the sense that node-GDV-similarity alone ($\alpha = 0$) is superior to the existing DP method (Supplementary Fig. S5). This is interesting because the two methods are somewhat similar. They both take into account graphlet degrees of two nodes in question. They differ in that DP considers only the 2-node graphlet and hence captures only the direct (1-deep) network neighborhoods of the nodes, whereas node-GDV-similarity considers all 2-5-node graphlets, thus capturing up to 4-deep node neighborhoods. Hence, in this context, including more network topology helps. (We compare the existing methods to our new graphlet-based methods in more detail in the following section.)

In general, using larger graphlets can increase LP accuracy (the following sections also confirm this). Since counting larger graphlets is computationally expensive compared to counting smaller graphlets (see Methods), whether it is worth including the extra topological information that is captured by the larger graphlets depends on how significant the improvement is.

New graphlet-based measures are superior over existing measures

Having examined different variations of the graphlet-based measures, we now compare these measures with the existing ones. Of all graphlet-based variations, we report the weighted version at $\alpha = 0.8$ when considering 3-5-node graphlets, since this version generally performs the best. The existing measures include DP, SN, JC, and AA.

Our graphlet-based method is superior to all existing methods in all three networks (Fig. 3 A). The p -value of the difference between LP accuracy of our method and any other method in Fig. 3 A is below 8.6×10^{-6} , 1.5×10^{-6} , and 1.2×10^{-6} for AP/MS, HC, and Y2H networks, respectively. It is worth noting that most of the methods perform quite well, reaching AUROCs of up to 0.99, 0.99, and 0.89 in AP/MS, HC, and Y2H networks, respectively. Whereas Fig. 3 A is for the lowest noise level, the results are similar for other noise levels (Supplementary Fig. S5). Interestingly, our graphlet-based measures further improve over the existing measures as the noise increases.

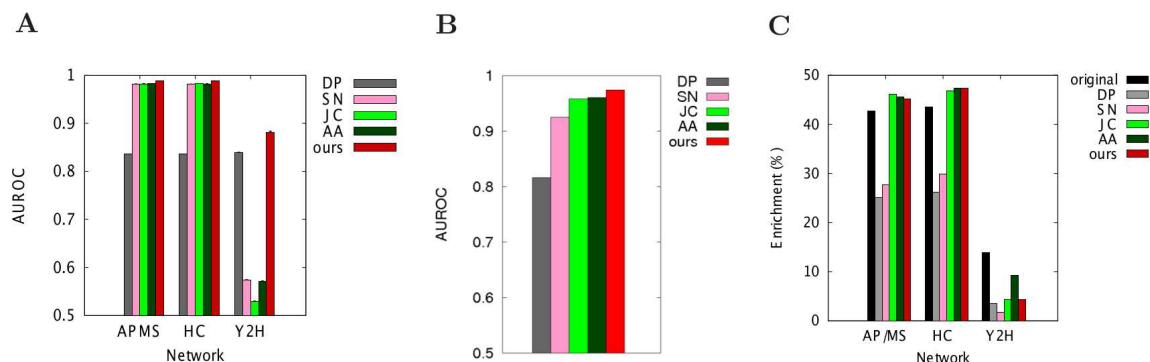


Figure 3. Comparison of different methods. Our best method (“ours”) is compared against existing methods (DP, SN, JC, and AA) in terms of: **A)** AUROCs for synthetically noised AP/MS, HC, and Y2H networks at 5% noise level; **B)** AUROCs for the HC network when using low confidence PPIs as the ground truth data; and **C)** GO enrichments of AP/MS, HC, and Y2H networks and their de-noised counterparts. “Ours” corresponds to using 3-5-node weighted graphlets at $\alpha = 0.8$ in panels A and C and using 3-4-node weighted graphlets at $\alpha = 0.4$ in panel B.

AUROC vs. precision-recall curves

Thus far, we have shown AUROC results. AUROCs are commonly used to evaluate methods over the entire [0%,100%] range of k [18], since the performance of each method can be summarized into a single number over the entire range, while precision-recall scores have to be shown for each value of k (see Methods). However, we find that the AUROC results are not necessarily consistent with precision-recall results. While in both AP/MS and HC networks all weighted graphlet-based measures are better than JC and AA with respect to AUROCs, JC and AA are better with respect to precision-recall curves (Fig. 3 A and Supplementary Fig. S5–S10). Further, for Y2H, we notice a different inconsistency: whereas AUROCs are high for the best-performing methods (Supplementary Fig. S5), precision-recall curves indicate poor performance of all methods, as precision is always low (Supplementary Fig. S8).

Even though optimizing AUROCs does not necessarily optimize precision-recall [7], the inconsistencies are alarming, and the LP community needs to be aware. We address this by also comparing the different methods with respect to biological correctness of their de-noised networks (see below). But first, we check whether results depend on the ground truth data, as follows.

Evaluating LP methods on HC network with respect to low-confidence PPI data

When we evaluate the LP methods on the HC network with low-confidence PPIs as the ground truth data, we find that:

1. As in the previous section (when evaluating LP methods by introducing synthetic noise into PPI networks), combining topological similarity and centrality of nodes to be linked improves LP accuracy. However, now α of 0.4 is the best overall instead of α of 0.8 (Supplementary Fig. S15 and S16): topological similarity is now *more* relevant than the number of shared graphlets.
2. As in the previous section, favoring denser graphlets improves LP accuracy for the best α (Supplementary Fig. S17).

3. As in the previous section, using more topology can improve LP accuracy (Supplementary Fig. S18). Using 3-4-node graphlets at the best α of 0.4 results in higher AUROC than using only 3-node graphlets at *any* α , and using 3-5-node graphlets at α of 0.8 results in higher AUROCs than using only 3-node graphlets or 3-4-node graphlets at the same α (Supplementary Fig. S18).
4. As in the previous section, our best graphlet-based measure in this context (using 3-4-node weighted graphlets at $\alpha = 0.4$) is superior to *all* existing measures (Fig. 3 B).
5. We again see inconsistencies between AUROC and precision-recall results (Fig. 3 B and Supplementary Fig. S19).

De-noising the PPI networks

Since both our new and the existing methods perform well on all networks with respect to AUROCs (Fig. 2 A and B and Supplementary Fig. S5), we use the overall best graphlet-based method (weighted 3-5-node graphlets at $\alpha = 0.8$) as well as DP, SN, JC, and AA to de-noise the networks. We score each node pair in a network, and we predict as edges in the de-noised network the top $k\%$ highest scoring node pairs. We choose k so that the number of edges in the de-noised network matches the number of edges in the original network. Depending on the network, k falls between 1% and 2%. We choose k in this way because most of the methods achieve the maximum F-score in this range of k (Supplementary Fig. S12-S14).

GO validation of de-noised networks

We validate biological correctness of the de-noised networks by computing the enrichment of all predicted edges in GO terms (see Methods and Fig. 3 C). When we de-noise AP/MS and HC networks, the enrichment is statistically significant for all methods (p -values $\leq 10^{-100}$). Our method as well as JC and AA *improve* the quality of the original AP/MS and HC networks. This is important, since the main goal of LP is to de-noise a network so that the de-noised network is more meaningful than the original one. While the GO enrichments are worse for the de-noised networks than for the original Y2H network, the enrichments are still statistically significant for our method, DP, JC, and AA (p -values ≤ 0.05). Interestingly, in this context, some shared neighbors-based measures slightly outperform our measure for AP/MS and Y2H networks, but our measure is marginally better for the HC network (Fig. 3 C).

Intersection of de-noised networks produced by different methods

Since we de-noise a network with multiple LP methods, we measure the intersections between the de-noised networks (Supplementary Fig. S20). The intersections are quite large between the shared neighbors-based methods and our method. JC is an exception, as it is somewhat different not only from our measure but also from other shared neighbors-based methods. Actually, our method is more similar to SN and AA than JC is. But interestingly, the intersections between the original networks and our method or JC are slightly larger than the intersections between the original networks and AA or SN, and all of these are much larger than the intersections between the original networks and DP.

Validation of de-noised networks on external PPI data

We aim to validate “new predicted edges” (predicted edges not present in the original network; Supplementary Table S1) by searching for them in BioGRID as an independent data source. We do this for the AP/MS network. Even though validation accuracy varies across the methods, all methods achieve statistically significant validation rates (p -values below 1×10^{-100}). Of the existing methods, only JC outperforms our method (Supplementary Fig. S21).

Concluding remarks

We tackle the problem of link prediction (LP) in the context of PPI network de-noising. We comprehensively study what is it in the PPI network topology around nodes in question that dictates whether the nodes should be linked. To evaluate whether nodes that share many neighbors and are thus close in the network are favored over distant nodes (as is the assumption of most of the existing LP methods), whether topological similarity between nodes in question has any effect, and how much of the network topology should be included, we had to propose new LP methods, since none of the existing methods allowed for answering all of these questions. Unlike the existing methods, our new methods allow for combining topological similarity of the nodes to be linked with the information about the size of their shared neighborhood, and they allow for varying the amount of network topology that is taken into account for LP. After we demonstrate via a thorough evaluation that our new methods are better than the existing methods, we use the methods to de-noise PPI networks. Importantly, the de-noised networks improve biological correctness of the original networks, which is the ultimate goal of LP in computational biology.

Acknowledgments

We thank Nicholas J. Taylor, an undergraduate Computer Science student at the University of Notre Dame, for implementing the common neighbors measures and running the corresponding analyses.

References

- [1] L. Adamic and E. Adar. Friends and neighbors on the Web. *Social Networks*, 25(3):211–230, 2003.
- [2] Michael Ashburner, Catherine A. Ball, Judith A. Blake, David Botstein, Heather Butler, J. Michael Cherry, Allan P. Davis, Kara Dolinski, Selina S. Dwight, Janan T. Eppig, Midori A. Harris, David P. Hill, Laurie Issel-Tarver, Andrew Kasarskis, Suzanna Lewis, John C. Matese, Joel E. Richardson, Martin Ringwald, Gerald M. Rubin, and Gavin Sherlock. Gene Ontology: tool for the unification of biology. *Nature Genetics*, 25(1):25–29, 2000.
- [3] A.L. Barabási and Z.N. Oltvai. Network biology: Understanding the cell’s functional organization. *Nature Reviews*, 5:101–113, 2004.
- [4] B. J. Breitkreutz, C. Stark, , T. Reguly, L. Boucher, A. Breitkreutz, M. Livstone, R. Oughtred, D. H. Lackner, J. Bahler, V. Wood, K. Dolinski, and M. Tyers. The BioGRID Interaction Database: 2008 update. *Nucleic Acids Research*, 36:D637–D640, 2008.
- [5] S. Brin and L. Page. The anatomy of a large-scale hypertextual Web search engine. *Computer Networks and ISDN Systems*, 30(1–7):107–117, 1998.
- [6] S.R. Collins, P. Kemmeren, X.C. Zhao, J.F. Greenblatt, F. Spencer, F.C.P. Holstege, J.S. Weissman, and N.J. Krogan. Toward a comprehensive atlas of the physical interactome of *saccharomyces cerevisiae*. *Molecular Cell Proteomics*, 6(3):439–450, 2007.
- [7] J. Davis and M. Goadrich. The relationship between Precision-Recall and ROC curves. In *Proceedings of the 23rd international conference on Machine learning*, pages 233–240. ACM, 2006.
- [8] A. M. Edwards, B. Kus, R. Jansen, D. Greenbaum, J. Greenblatt, and M. Gerstein. Bridging structural biology and genomics: assessing protein interaction data with known complexes. *Trends Genet*, 18:529–36, 2002.

- [9] L. Getoor and C.P. Diehl. Link mining: a survey. *SIGKDD Explorations Newsletter*, 7(2):3–12, 2005.
- [10] L. Giot, J.S. Bader, C. Brouwer, A. Chaudhuri, B. Kuang, Y. Li, Y.L. Hao, C.E. Ooi, B. Godwin, E. Vitols, G. Vijayadamodar, P. Pochart, H. Machineni, M. Welsh, Y. Kong, B. Zerhusen, R. Malcolm, Z. Varrone, A. Collis, M. Minto, S. Burgess, L. McDaniel, E. Stimpson, F. Spriggs, J. Williams, K. Neurath, N. Ioime, M. Agee, E. Voss, K. Furtak, R. Renzulli, N. Aanensen, S. Carrolla, E. Bickelhaupt, Y. Lazovatsky, A. DaSilva, J. Zhong, C.A. Stanyon, R.L. Jr Finley, K.P. White, M. Braverman, T. Jarvie, S. Gold, M. Leach, J. Knight, R.A. Shimkets, M.P. McKenna, J. Chant, and J.M. Rothberg. A protein interaction map of *Drosophila melanogaster*. *Science*, 302(5651):1727–1736, 2003.
- [11] J.D.H. Han, D. Dupuy, N. Bertin, M.E. Cusick, and Vidal. M. Effect of sampling on topology predictions of protein-protein interaction networks. *Nature Biotechnology*, 23:839–844, 2005.
- [12] H. Ho, T. Milenković, V. Memisevic, J. Aruri, N. Pržulj, and A. Ganesan. Protein interaction network uncovers melanogenesis regulatory network components within functional genomics datasets. *BMC Systems Biology*, 4(84), 2010.
- [13] O. Kuchaiev, T. Milenković, V. Memišević, W. Hayes, and N. Pržulj. Topological network alignment uncovers biological function and phylogeny. *Journal of the Royal Society Interface*, 7:1341–1354, 2010.
- [14] O. Kuchaiev and N. Pržulj. Integrative network alignment reveals large regions of global network similarity in yeast and human. *Bioinformatics*, 27(10):1390–1396, 2011.
- [15] O. Kuchaiev, M. Rasajski, D. Higham, and N. Pržulj. Geometric de-noising of protein-protein interaction networks. *PLoS Computational Biology*, 5:e1000454, 2009.
- [16] D. Liben-Nowell and J. Kleinberg. The link prediction problem for social networks. In *Proceedings of the twelfth international conference on Information and knowledge management*, CIKM 2003, pages 556–559. ACM, 2003.
- [17] D. Liben-Nowell and J. Kleinberg. The link-prediction problem for social networks. *J. Am. Soc. Inf. Sci.*, 58(7):1019–1031, 2007.
- [18] R.N. Lichtenwalter, J.T. Lussier, and N.V. Chawla. New perspectives and methods in link prediction. In *Proceedings of the 16th ACM SIGKDD International Conference on Knowledge Discovery and Data Mining*, pages 243–252. ACM, 2010.
- [19] Ryan N. Lichtenwalter and Nitesh V. Chawla. Vertex collocation profiles: subgraph counting for link analysis and prediction. In *Proceedings of the 21st international conference on World Wide Web*, WWW '12, pages 1019–1028, New York, NY, USA, 2012. ACM.
- [20] L. Lü and T. Zhou. Link prediction in complex networks: A survey. *Physica A: Statistical Mechanics and its Applications*, 390(6):1150–1170, 2010.
- [21] D. Marcus and Y. Shavitt. RAGE - A rapid graphlet enumerator for large networks. *Computer Networks*, 56(2):810 – 819, 2012.
- [22] V. Memisević, T. Milenković, and N. Pržulj. An integrative approach to modeling biological networks. *Journal of Integrative Bioinformatics*, 7(3):120, 2010.
- [23] T. Milenković, I. Filippis, M. Lappe, and N. Pržulj. Optimized null model for protein structure networks. *PLoS ONE*, 4(6):e5967, 2009.

- [24] T. Milenković, J. Lai, and N. Pržulj. GraphCrunch: a tool for large network analyses. *BMC Bioinformatics*, 9(70), 2008.
- [25] T. Milenković, V. Memisević, A. K. Ganesan, and N. Pržulj. Systems-level cancer gene identification from protein interaction network topology applied to melanogenesis-related interaction networks. *Journal of the Royal Society Interface*, 7:423–437, 2010.
- [26] T. Milenković, V. Memisević, A. Bonato, and N. Pržulj. Dominating biological networks. *PLoS ONE*, 6(8):e23016, 2011.
- [27] T. Milenković, W.L. Ng, W. Hayes, and N. Pržulj. Optimal network alignment with graphlet degree vectors. *Cancer Informatics*, 9:121–137, 2010.
- [28] T. Milenković and N. Pržulj. Uncovering biological network function via graphlet degree signatures. *Cancer Informatics*, 6:257–273, 2008.
- [29] M.E.J. Newman. Clustering and preferential attachment in growing networks. *Phys Rev E*, 64, 2001.
- [30] N. Pržulj. Biological network comparison using graphlet degree distribution. *Bioinformatics*, 23:e177–e183, 2007.
- [31] N. Pržulj, D. G. Corneil, and I. Jurisica. Modeling interactome: Scale-free or geometric? *Bioinformatics*, 20(18):3508–3515, 2004.
- [32] M.J. Rattigan and D. Jensen. The case for anomalous link discovery. *SIGKDD Explorations Newsletter*, 7(2):41–47, 2005.
- [33] G. Salton and M. McGill. *Introduction to modern information retrieval*. McGraw-Hill Book Company, New York, 1984.
- [34] Ömer Sinan Saraç, Vera Pancaldi, Jrg Böhler, and Andreas Beyer. Topology of functional networks predicts physical binding of proteins. *Bioinformatics*, 28(16):2137–2145, 2012.
- [35] R. Sharan and T. Ideker. Modeling cellular machinery through biological network comparison. *Nature Biotechnology*, 24(4):427–433, Apr 2006.
- [36] R. Sharan and T. Ideker. Protein networks in disease. *Genome Research*, 18:644–652, 2008.
- [37] R. Sharan, I. Ulitsky, and R. Shamir. Network-based prediction of protein function. *Molecular Systems Biology*, 3(88):1–13, 2007.
- [38] N. Simonis, J. F. Rual, A. R. Carvunis, M. Tasan, I. Lemmens, T. Hirozane-Kishikawa, T. Hao, J. M. Sahalie, K. Venkatesan, F. Gebreab, S. Cevik, N. Klitgord, C. Fan, P. Braun, N. Li, N. Ayivi-Guedehoussou, E. Dann, N. Bertin, D. Szeto, A. Dricot, M. A. Yildirim, C. Lin, A. S. de Smet, H. L. Kao, C. Simon, A. Smolyar, J. S. Ahn, M. Tewari, M. Boxem, S. Milstein, H. Yu, M. Dreze, J. Vandenhoute, K. C. Gunsalus, M. E. Cusick, D. E. Hill, J. Tavernier, F. P. Roth, and M. Vidal. Empirically controlled mapping of the *Caenorhabditis elegans* protein-protein interactome network. *Nature methods*, 6(1):47–54, 2009.
- [39] R.W. Solava, R.P. Michaels, and T. Milenković. Graphlet-based edge clustering reveals pathogen-interacting proteins. *Bioinformatics*, 18(28):i480–i486, 2012. Also, in Proceedings of the *11th European Conference on Computational Biology (ECCB)*, Basel, Switzerland, September 9-12, 2012 (acceptance rate: 14%).

- [40] U. Stelzl, U. Worm, M. Lalowski, C. Haenig, F.H. Brembeck, H. Goehler, M. Stroedicke, M. Zenkner, A. Schoenherr, S. Koeppen, J. Timm, S. Mintzlauff, C. Abraham, N. Bock, S. Kietzmann, A. Goedde, E. Toksoz, A. Droege, S. Krobitsch, B. Korn, W. Birchmeier, H. Lehrach, and E.E. Wanker. A human protein-protein interaction network: A resource for annotating the proteome. *Cell*, 122:957–968, 2005.
- [41] M.P.H. Stumpf, C. Wiuf, and R.M. May. Subnets of scale-free networks are not scale-free: Sampling properties of networks. *PNAS*, 102:4221–4224, 2005.
- [42] O. Vanunu, O. Magger, E. Ruppin, T. Shlomi, and R. Sharan. Associating genes and protein complexes with disease via network propagation. *PLoS Computational Biology*, 6:e1000641, 2010.
- [43] K. et al. Venkatesan. An empirical framework for binary interactome mapping. *Nature Methods*, 6(1):83–90, 2009.
- [44] C. von Mering, R. Krause, B. Snel, M. Cornell, S. G. Oliver, S. Fields, and P. Bork. Comparative assessment of large-scale data sets of protein-protein interactions. *Nature*, 417(6887):399–403, 2002.
- [45] D.J. Watts and S.H. Strogatz. Collective dynamics of 'small-world' networks. *Nature*, 393:440–442, 1998.
- [46] S.J. Wodak, S. Pu, J. Vlasblom, and B. Seraphin. Challenges and rewards of interaction proteomics. *Molecular Cell Proteomics*, 8(1):3–18, 2009.
- [47] H. et al. Yu. High-quality binary protein interaction map of the yeast interactome networks. *Science*, 322:104–110, 2008.